

# Critical behavior of the metallic triangular-lattice Heisenberg antiferromagnet PdCrO<sub>2</sub>

Hiroshi Takatsu,<sup>1,\*</sup> Hideki Yoshizawa,<sup>2</sup> Shingo Yonezawa,<sup>1</sup> and Yoshiteru Maeno<sup>1</sup>

<sup>1</sup>*Department of Physics, Graduate School of Science, Kyoto University, Kyoto 606-8502, Japan*

<sup>2</sup>*Neutron Science Laboratory, Institute for Solid State Physics,  
The University of Tokyo, Tokai Ibaraki 319-1106, Japan*

(Dated: August 8, 2018)

We report physical properties of the conductive magnet PdCrO<sub>2</sub> consisting of a layered structure with a triangular lattice of Cr<sup>3+</sup> ions ( $S = 3/2$ ). We confirmed an antiferromagnetic transition at  $T_N = 37.5$  K by means of specific heat, electrical resistivity, magnetic susceptibility, and neutron scattering measurements. The critical behavior in the specific heat persists in an unusually wide temperature range above  $T_N$ . This fact implies that spin correlations develop even at much higher temperature than  $T_N$ . The observed sub-linear temperature dependence of the resistivity above  $T_N$  is also attributed to the short-range correlations among the frustrated spins. While the critical exponent for the magnetization agrees reasonably with the prediction of the relevant model, that for the specific heat evaluated in the wide temperature range differs substantially from the prediction.

PACS numbers: 74.25.Ha, 75.40.Cx, 84.37.+q

## I. INTRODUCTION

Geometrically frustrated spin systems have attracted much attention for the realization of novel ground states with unconventional order parameters. Especially, antiferromagnetically interacting spins on two-dimensional (2D) triangular lattices (TL) are actively investigated because the simple triangular arrangement of spins gives rise to various ground states depending on the nature of the spins.<sup>1,2,3,4,5,6,7</sup> One remarkable example is a continuous spin system such as XY or Heisenberg magnets.<sup>4,5,6,7,8,9,10,11,12,13</sup> For such systems, it is predicted that the frustration is partially relaxed by forming a local 120° spin structure. The short-range spin correlations produces a new degree of freedom called the vector chirality. Interestingly, the vector chirality may exhibit a long range order at a finite temperature although the spins are *not* long-range ordered. However, it is difficult to detect the chirality order directly in real materials because many of them exhibit static long-range spin order due to additional interactions (e.g. inter-layer interactions) above their predicted chirality-order temperature. Nevertheless, it is expected that the proximity to chirality order affects the critical behavior of physical properties near a magnetic phase transition.<sup>13,14,15</sup> Indeed, e.g., the 2D triangular Heisenberg antiferromagnetic (THAF) compounds, VX<sub>2</sub> ( $X = \text{Cl, Br}$ ) exhibit an unusual critical behavior with characteristic critical exponents.<sup>16,17,18</sup> Therefore, a detailed investigation of the critical behavior may reveal the interplay between spin and vector chirality.

Most of the 2D THAF compounds are insulators or semiconductors. Therefore, the magnetic properties of 2D metallic THAF compounds have not been sufficiently clarified. In order to reveal the intrinsic interaction of the conduction electrons with frustrated spin moments, it is desirable to investigate a clean metallic THAF compound without disorder introduced by chemical doping.

We studied the 2D THAF oxide PdCrO<sub>2</sub> (Cr<sup>3+</sup>,  $S = 3/2$ ) and revealed that it exhibits metallic conductivity without chemical doping down to low temperatures. Thus, we believe that this oxide is one of the simplest and most suitable systems for the investigation of the interplay between conduction elec-

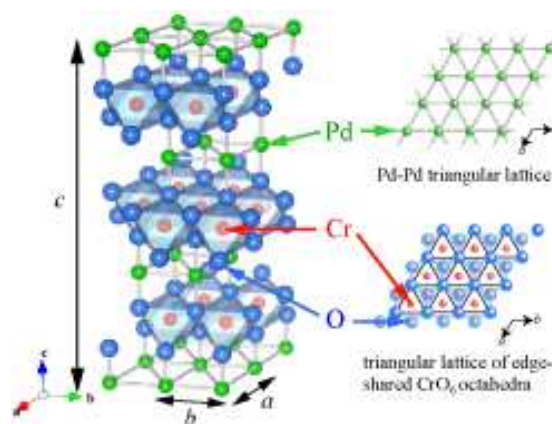


FIG. 1: (Color online) Crystal structure of PdCrO<sub>2</sub>. This structure consists of alternating stacks of a triangular lattice of palladium and a triangular lattice of edge-shared CrO<sub>6</sub> octahedra. These drawings were produced using the software VESTA.<sup>19</sup>

trons and frustrated magnetism, as well as the involvement of the vector chirality.

PdCrO<sub>2</sub> crystallizes in the delafossite structure with the space group  $R\bar{3}m$  ( $D_{3d}^5$ ). This structure is closely related to the ordered rock-salt structure of ACrO<sub>2</sub> ( $A = \text{Li, Na, K}$ ).<sup>20</sup> However, they exhibit a different stacking sequence of the respective oxide and metal-ion layers in the unit cell. In the delafossite structure, the noble-metal ions such as Pd<sup>1+</sup> are linearly coordinated by two oxygen ions along the  $c$  axis like a dumbbell, whereas in the ordered rock-salt structure, the alkali-metal ions  $A^{1+}$  are zigzag connected to oxygen ions. The lattice parameters of PdCrO<sub>2</sub> at 25°C are  $a = b = 2.930$  Å and  $c = 18.087$  Å.<sup>21</sup> The temperature dependence of the magnetic susceptibility starts to deviate from a Curie-Weiss behavior below room temperature with a broad peak at about 60 K.<sup>22</sup> The Weiss temperature  $\theta_W$  and the effective moment  $\mu_{\text{eff}}$  were reported to be  $\theta_W \approx -500$  K and  $\mu_{\text{eff}} \approx 4.1\mu_B$ . Moreover, a powder neutron scattering study down to 8 K revealed a mag-

netic transition around  $T_N = 40$  K, leading to a  $120^\circ$  spin structure.<sup>23</sup> The frustration parameter  $f \equiv |\theta_W|/T_N \approx 13$  indicates strong spin frustration. To our knowledge the electrical resistivity and the specific heat of this compound have not been reported before our investigation.<sup>24</sup> We note that the isostructural non-magnetic compound PdCoO<sub>2</sub> exhibits a metallic temperature dependence of the resistivity down to 20 mK, which is attributed to the Pd 4d<sup>9</sup> electrons. It is also revealed that the high-frequency phonons play an essential role in the temperature dependence of the resistivity and specific heat.<sup>25</sup>

This paper reports the critical behavior of metallic PdCrO<sub>2</sub> around its  $T_N$  investigated by detailed measurements of the specific heat. We found that the resistivity of PdCrO<sub>2</sub> exhibits an unusual sub-linear temperature dependence at temperatures above  $T_N$ . We also revealed the critical behavior in the specific heat persisting in the temperature range where the  $T$ -sub-linear resistivity is found. These results imply that the short-range correlation of frustrated spins gives rise to such characteristic behavior in PdCrO<sub>2</sub>.

## II. EXPERIMENTAL

Powder samples of PdCrO<sub>2</sub> were obtained by the reaction,  $\text{Pd} + \text{PdCl}_2 + 2\text{LiCrO}_2 \rightarrow 2\text{PdCrO}_2 + 2\text{LiCl}$ .<sup>21,22</sup> We first prepared LiCrO<sub>2</sub> by reacting the stoichiometric mixture of LiCO<sub>3</sub> (99.99%, Aldrich Chemical Co.) and Cr<sub>2</sub>O<sub>3</sub> (99.99%, Rare Metallic Co. Ltd.) at 850°C in an alumina crucible for 24 hours. We added Pd powder (99.99%, Furuuchi Chem. Co.) and PdCl<sub>2</sub> powder (99.999%, Aldrich Chemical Co.) to the LiCrO<sub>2</sub> powder, and ground the mixture in a mortar for 30 – 60 minutes. It was then heated to 790°C and kept for 96 hours in evacuated quartz tubes. The obtained samples were washed with aqua regia and distilled water to remove LiCl, the remaining Pd, and other by-products. The samples were characterized by using powder X-ray diffraction (XRD) with CuK <sub>$\alpha$</sub> 1 radiation and energy dispersive X-ray analysis (EDX). The XRD pattern indicated no impurity phase. The EDX spectra yielded a composition ratio of Pd and Cr of Pd/Cr = 1.07, suggesting stoichiometry within the experimental resolution. However, the sample used in the powder neutron scattering experiment contained an impurity phase as indicated by a neutron diffraction peak at  $2\theta \approx 53^\circ$ , see Fig. 5. Since powder neutron diffraction requires a large amount of sample, we could not completely remove the impurity phase for that sample.

Specific heat was measured by applying a thermal relaxation method with a commercial calorimeter (Quantum Design, PPMS) from 250 K to 0.35 K, using pressed pellets sintered at 700 °C for 12 – 24 hours. Around the transition temperature  $T_N$  we carefully took data points in 0.01 K intervals. The temperature heating width  $\Delta T$  during each measurement was chosen to be  $\Delta T \leq 0.08$  K. Note that a specific-heat measurement using the thermal relaxation method requires special attention to  $\Delta T$  in the immediate vicinity of a phase transition because the obtained specific heat value is a certain average of  $C_P(T)$  in the temperature interval from  $T$  to  $T + \Delta T$ .

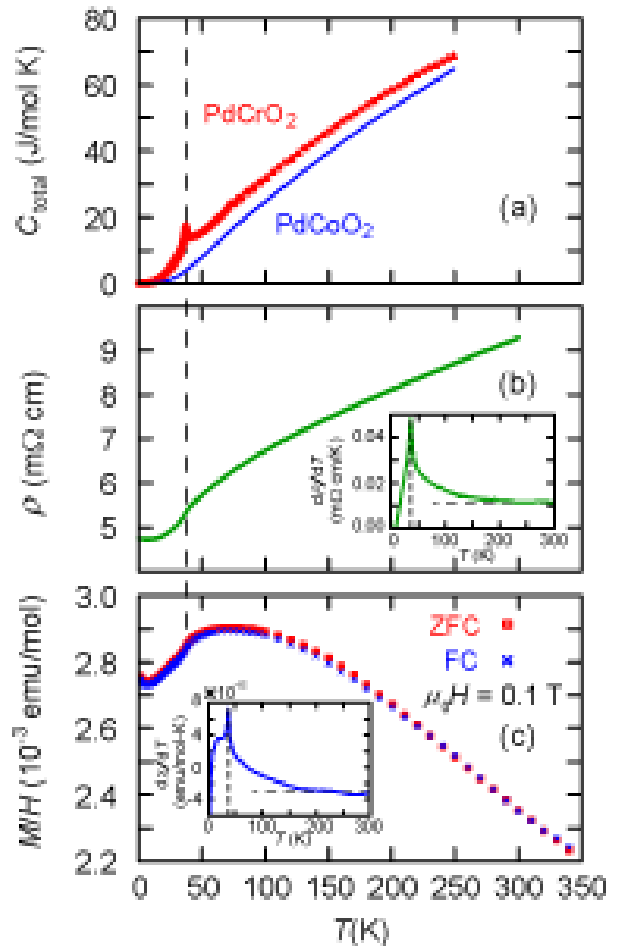


FIG. 2: (Color online) Temperature dependence of (a) the specific heat, (b) electrical resistivity, and (c) magnetic susceptibility of PdCrO<sub>2</sub>. The antiferromagnetic transition gives rise to anomalies at  $T_N = 37.5$  K in all these quantities. The solid line in (a) represents the specific heat of the isostructural but non-magnetic compound, PdCoO<sub>2</sub> [Ref. 25]. The insets in (b) and (c) indicate the temperature derivatives of the resistivity and susceptibility. They exhibit a clear peak at  $T_N$ . Fig. 2(c) includes results of both zero-field cooling and field-cooling measurements of the magnetic susceptibility at 0.1 T.

Electrical resistivity was measured with either AC or DC four-probe method from 300 K to 0.35 K. In the temperature range from 2.0 K to 0.35 K, a <sup>3</sup>He refrigerator (Oxford Instruments, Heliox) was used. Gold wires were attached with silver paste to rectangular samples cut out from pellets.

DC magnetization was measured with a commercial SQUID magnetometer (Quantum Design, MPMS) from 300 K to 1.8 K in magnetic fields  $\mu_0 H$  between 0.002 T and 7 T. The field dependence of the DC magnetization was also measured from  $-7$  T to 7 T at 4.2 K.

The powder neutron scattering measurements were performed in zero field on the triple axis spectrometer GPTAS-4G at JRR-3. A pyrolytic graphite (002) reflection was used for the monochromator. Higher-order neutrons were removed by a pyrolytic graphite filter. The neutron wave length was

fixed to  $\lambda = 2.3475 \text{ \AA}$ , and a collimation of  $40' - 80' - 40' - 80'$  was chosen. The linear dimensions of the pelletized sample used was  $23 \text{ mm} \times \phi 9 \text{ mm}$  and it was mounted in a  $^3\text{He}$  cryostat with a closed-cycle  $^4\text{He}$  refrigerator. The present measurements extend to temperatures as low as 0.8 K, compared with the previous report, 8 K.<sup>23</sup>

### III. RESULTS

#### A. Specific heat

The temperature dependence of the specific heat is presented in Fig. 2(a). The specific heat exhibits a clear peak at  $T_N = 37.5 \text{ K}$ , at which the temperature derivative of the resistivity ( $d\rho/dT$ ) and that of the susceptibility ( $d\chi/dT$ ) also exhibit a clear peak. Since previous<sup>23</sup> and the present neutron scattering measurements have also revealed magnetic Bragg peaks at low temperatures, the results indicate that the static long-range spin-order occurs at  $T_N$ . It should be noted that the total specific heat ( $C_P$ ) of  $\text{PdCrO}_2$  is noticeably larger than that of the isostructural non-magnetic  $\text{PdCoO}_2$  even at 250 K, although it is often expected that  $C_P$  of a magnetic compound approaches that of the non-magnetic counterpart at high temperatures. This difference is mainly attributed to the difference of the Einstein modes in the phononic contribution ( $C_{\text{ph}}$ ).

In order to estimate the magnetic specific heat for  $\text{PdCrO}_2$  ( $C_{\text{mag}}$ ), we subtracted the phononic contribution ( $C_{\text{ph,Cr}}$ ) and the electronic contribution ( $C_{\text{ele}}$ ) from  $C_P$  of  $\text{PdCrO}_2$ . The phononic contribution  $C_{\text{ph,Cr}}$  was estimated by multiplying  $C_{\text{ph}}$  of  $\text{PdCoO}_2$  by a constant such that it approaches  $C_P$  of  $\text{PdCrO}_2$  at high temperatures; we used 1.09 for this constant. This model empirically corrects for the number of the Debye modes while effectively incorporating the reduction of the Einstein frequencies. The electronic contribution  $C_{\text{ele}}$  ( $= \gamma_{\text{ele}} T$ ) was estimated by fitting the relation

$$C_P - C_{\text{ph,Cr}} = C_{\text{ele}} + C_{\text{mag}} \\ = \gamma_{\text{ele}} T + A_{\text{mag}} T^h \quad (1)$$

to the data in the temperature interval between 0.35 K and 4.0 K. In Eq. (1),  $\gamma_{\text{ele}}$  denotes the electronic specific-heat coefficient, and  $C_{\text{mag}} = A_{\text{mag}} T^h$  describes the magnon contribution much below  $T_N$ .<sup>26</sup> It is known that  $h$  fulfills the relation  $h = d/\varepsilon$ , where  $d$  is the dimensionality of the magnon excitation and  $\varepsilon$  is a parameter related to the type of the magnetic order ( $\varepsilon = 1$  refers to AF order,  $\varepsilon = 2$  to ferromagnetic order).<sup>26</sup> The coefficient  $A_{\text{mag}}$  is related to the spin velocity  $v_S$  in the long-range-ordered state.<sup>27,28</sup>

The fitting yields  $\gamma_{\text{ele}} = 1.4 \pm 0.2 \text{ mJ/mol-K}^2$ ,  $h = 2.0 \pm 0.1$ , and  $A_{\text{mag}} = 1.2 \text{ mJ/mol-K}^3$ . At 2 K, the magnitudes of the two terms (electronic and magnetic) are comparable, and the phonon contribution is only about 5% of the total specific heat. Thus, the electronic contribution can be evaluated with sufficient precision and accuracy. The value of  $\gamma_{\text{ele}}$  is similar to the value found for non-magnetic  $\text{PdCoO}_2$  ( $\gamma_{\text{ele}} = 1.28 \text{ mJ/mol-K}^2$ ),<sup>25</sup> implying that the mass enhancement due to interactions between electrons and magnetic moments is not strong. The observed  $T^2$  dependence of  $C_{\text{mag}}$  is

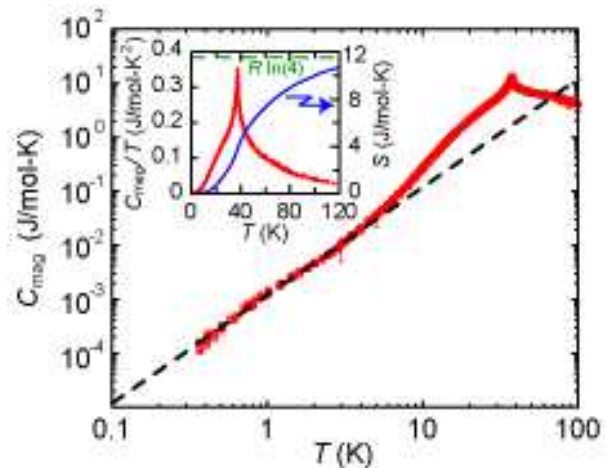


FIG. 3: (Color online) Temperature dependence of the magnetic specific heat of  $\text{PdCrO}_2$ . These data were obtained by subtracting the contribution of phonons and conduction electrons. The phononic contribution was estimated from the specific heat of isostructural but non-magnetic  $\text{PdCoO}_2$ . The solid line is a fit to the data  $\sim T^{2.0 \pm 0.1}$  indicating a realization of the 2D-magnon excitation in an antiferromagnetically spin-ordered state. In the inset the temperature dependence of the magnetic specific heat divided by temperature  $C_{\text{mag}}/T$  is shown. A sharp peak clearly indicates the transition at  $T_N = 37.5 \text{ K}$ .

consistent with the theoretical prediction of the  $T$ -dependence of the specific heat due to 2D-magnon excitations in an AF ordered state, i.e.  $d = 2$  and  $\varepsilon = 1$ . The spin velocity  $v_S$  is estimated to be  $v_S \approx 3200 \text{ m/s}$  from the relation  $v_S = [3.606 \sqrt{3}R/2\pi A_{\text{mag}}]^{1/2} (ak_B/\hbar)$ , which is applicable to the magnetic order with 2D-magnon excitations in a TL magnet.<sup>28</sup>

The estimated  $C_{\text{mag}}$  ( $= C_P - \gamma_{\text{ele}} T - C_{\text{ph}}$ ) is displayed in Fig. 3 on a logarithmic scale (main panel), which indicates a clear  $T^2$  dependence below 4 K. Interestingly, a small hump structure is observed at about 20 K below the AF transition (inset of Fig. 3). A similar hump is also observed in  $\text{CuCrO}_2$  and some frustrated spinel magnets.<sup>29,30</sup> A recent theory points out that such a hump in  $C_{\text{mag}}$  below the magnetic transition originates from quantum fluctuations of frustrated spins.<sup>31</sup>

The magnetic entropy at  $T_N$  evaluated from the integration of  $C_{\text{mag}}(T)/T$  from 0.35 K is  $3.9 \pm 0.1 \text{ J/mol-K}$ . This value is remarkably small because it is only one third of the expected entropy for a system with  $S = 3/2$  localized spins:  $R \ln(2S + 1) = 11.53 \text{ J/mol-K}$ . We have confirmed that the value of the magnetic entropy at  $T_N$  is not affected by the choice of a model for the estimation of  $C_{\text{ph}}$ .<sup>24</sup> The inset of Fig. 3 indicates that the entropy release persists to much higher temperatures. This fact implies that strong short-range spin correlations persist to temperatures much above  $T_N$ .

Figure 4 shows the behavior of  $C_{\text{mag}}$  in the critical region above and below  $T_N$ , displayed against the reduced temperature  $t \equiv |T/T_N - 1|$ . The behavior in the critical region above  $T_N$  surprisingly extends up to about  $t \approx 0.6$ ; for ordinary magnets, such behavior is observed only up to  $t \approx 0.1$ .<sup>32,33</sup> This behavior implies again that the magnetic correlations start to

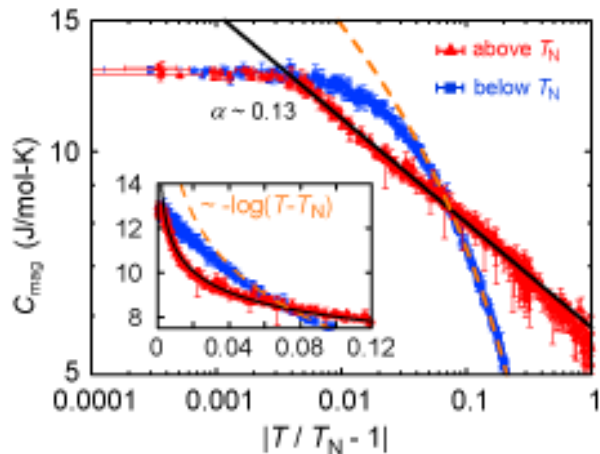


FIG. 4: (Color online) Critical behavior of the magnetic specific heat. The temperature range in which the critical behavior is observed extends up to around  $T/T_N - 1 = 0.6$  (around 60 K). The critical exponents  $\alpha^\pm$  are estimated as  $\alpha^+ = 0.13 \pm 0.02$  above  $T_N$  and as  $\alpha^- = 0$  below  $T_N$ .

develop from temperatures much higher than  $T_N$ . In order to estimate the critical exponents above and below  $T_N$ , we performed the fitting to the data with the relation,

$$C_{\text{mag}} = A^\pm |T/T_N - 1|^{-\alpha^\pm}, \quad (2)$$

where  $\alpha^+$  and  $\alpha^-$  denote exponents above and below  $T_N$ , and  $A^\pm$  represents respective coefficients. The resulting exponent is  $\alpha^+ = 0.13 \pm 0.02$  ( $0.005 < t \leq 0.6$ ) above  $T_N$ . In the vicinity of  $T_N$ , we reproducibly observed saturation of the divergence in several samples investigated in this study. Such saturation is often observed in other magnets as well.<sup>34</sup> Anticipating another value of  $\alpha$  in the conventional critical region, we fitted Eq.(2) to the data between 0.005 and 0.1. The obtained value  $\alpha^+ = 0.14 \pm 0.02$  is essentially the same as that obtained in the wide temperature range. This indicates, as it is also evident from Fig. 4, that the critical behavior near  $T_N$  persists to high temperatures. For temperatures below  $T_N$ , the critical behavior is weaker than  $\log(t)$ . It is known that the three cases, a logarithmic divergence, a cusp and a jump at  $T_N$ , are represented by the critical exponent  $\alpha = 0$ . Thus we assign  $\alpha^- = 0$  for the cusp observed in PdCrO<sub>2</sub>. We will further discuss the critical exponents  $\alpha^\pm$  in Sec. IV.

### B. Electrical resistivity

In Fig. 2(b) the electrical resistivity of PdCrO<sub>2</sub> between 300 K and 0.35 K is shown. The anomaly due to the AF transition is observed at temperatures centered around  $37.5 \pm 0.5$  K at which  $d\rho/dT$  exhibits a clear sharp peak in agreement with the specific-heat data. The resistivity exhibits a metallic temperature dependence down to 0.35 K but a very weak upturn of about 0.2% below 7 K. This weak upturn is attributed to a weak localization of conduction electrons due to grain bound-

aries in the pelletized samples, because no anomaly was found at that temperature in other quantities.

By fitting the formula  $\rho(T) = A + BT^n$  to the data below and above  $T_N$ , we obtained  $n = 2.9 \pm 0.1$  ( $10 \text{ K} < T < 35 \text{ K}$ ) and  $n = 0.34 \pm 0.05$  ( $38 \text{ K} < T < 150 \text{ K}$ ). Below the transition temperature, the behavior in PdCrO<sub>2</sub> is consistent with that of ordinary magnetic metals with localized moments, which are known to exhibit such super-linear temperature dependence with  $n > 1$ .<sup>35,36,37</sup> However, above  $T_N$ , the observed sub-linear temperature dependence with  $n < 1$  is clear contrast to the resistivity of ordinary magnetic metals.<sup>38,39</sup> We will discuss the origin of this unusual  $T$ -sub-linear resistivity observed in PdCrO<sub>2</sub> in Sec. IV.

We note here that there exists sample dependence in the absolute values of the resistivity, probably due to the fragility of the samples. However, the qualitative behavior of the resistivity is consistent for all the samples investigated.

### C. Magnetic susceptibility

The results of the DC magnetic susceptibility ( $M/H = \chi$ ) for zero-field cooling (ZFC) and field cooling (FC) runs at 0.1 T from 350 K to 1.8 K are shown in Fig. 2(c). The susceptibility  $\chi$  continuously increases with decreasing temperature. Below about 200 K it starts to deviate from ordinary Curie Weiss behavior. It exhibits a broad peak around 60 K as previously reported.<sup>22</sup> Such behavior is also reported for other 2D-THAF compounds, e. g., VCl<sub>2</sub> [Ref. 40] and ACrO<sub>2</sub> ( $A=\text{Li, Na}$ ),<sup>41,42</sup> indicating a development of 2D short-range spin correlations with decreasing temperature. At  $T_N$ ,  $\chi$  exhibits a continuous anomaly and  $d\chi/dT$  exhibits a clear peak. Moreover,  $d\chi/dT$  exhibits a shoulder structure around 20 K (the inset of Fig 2(c)), at which  $C_{\text{mag}}$  also exhibits the hump.

Fitting  $\chi(T) = \chi_0 + C/(T - \theta_W)$  to the corrected data in the temperature interval 250 K to 350 K, we obtained the effective moment to be  $\mu_{\text{eff}} = 3.8 - 4.1\mu_B$  and the Weiss temperature to be  $\theta_W \simeq -500$  K, which are consistent with the earlier report.<sup>22</sup>

### D. Neutron scattering

Powder neutron diffraction patterns at several temperatures in zero field are shown in Fig. 5. Below  $T_N$ , we observed magnetic Bragg peaks. The observed magnetic Bragg peaks are rather broad, implying short coherence of the long-range order. The peak positions can be labeled as  $(\frac{1}{3}, \frac{1}{3}, l)$  and  $(\frac{2}{3}, \frac{2}{3}, l)$  with  $l = 0, \frac{1}{2}, 1, \frac{3}{2}, 2 \dots$ , which are consistent with the peaks for the 120° spin structure as previously reported by Mekata *et al.*<sup>23</sup> The intensity of each peak is also consistent with their report. From the weaker relative intensity of the  $(\frac{1}{3}, \frac{1}{3}, 0)$  peak compared with that of the  $(\frac{1}{3}, \frac{1}{3}, 1)$  peak, they deduced that the spins lie in the  $ab$  plane. Interestingly, magnetic Bragg peaks with half-integer  $l$  are observed in addition to the integer  $l$  peaks. The spectrum observed in the delafossite PdCrO<sub>2</sub> resembles that of LiCrO<sub>2</sub> in the ordered rock-salt structure [Ref. 43], but in contrast with that of CuCrO<sub>2</sub> in the delafossite

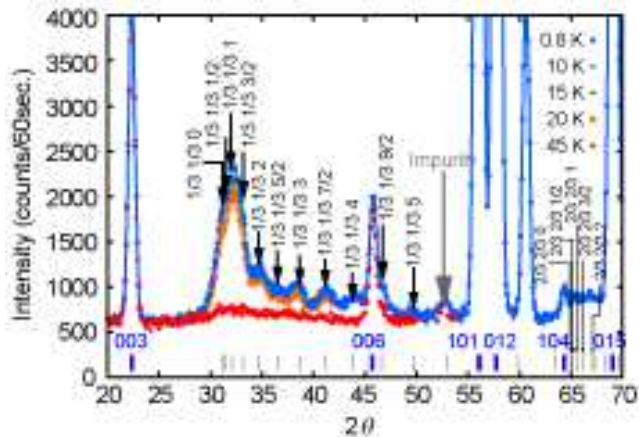


FIG. 5: (Color online) Powder neutron diffraction patterns obtained at 0.8 K, 10 K, 15 K, 20 K, and 45 K in zero field with the counting time of 60 sec. for each data point. The peak positions are indexed. The observed magnetic Bragg peaks are clearly broader than the instrument resolution. The diffuse scattering feature centered around  $\theta \sim 32^\circ$  remains visible above  $T_N$ . An impurity peak was detected at  $2\theta = 53^\circ$ , see text.

structure [Ref. 44]. The observation of the half integer peaks suggests a  $\text{LiCrO}_2$ -type magnetic structure, which is believed to have two independent propagation vectors.<sup>43</sup> Alternatively, the spectra are equally well interpreted in terms of two kinds of magnetic domains with  $l = \text{integers}$  and  $l = \text{half-integers}$ . In this case, the volume fractions of the domains contained in our sample are nearly the same.

As seen in Fig. 5, the diffuse scattering feature between  $2\theta = 30^\circ$  and  $44^\circ$  is still visible at 45 K (above  $T_N = 37.5$  K). This result indicates that strong short-range spin correlation is present at temperatures substantially higher than  $T_N$ . Note that such a diffuse component above  $T_N$  was also observed in other triangular lattice chromium compounds  $\text{CuCrO}_2$ ,  $\text{LiCrO}_2$ , and  $\text{NaCrO}_2$ <sup>44,45</sup>.

The temperature dependence of the peak intensity at several  $q$  positions is shown in Fig 6. Since the peak intensity at  $(\frac{1}{3}, \frac{1}{3}, 4)$  is very weak, the counting time was doubled to 180 seconds compared to the other measurements. All the intensities exhibit a gradual increase with decreasing temperature and no anomaly around 7 K or 20 K. These results indicate that there are no significant changes in the magnetic structure at low temperatures.

We estimated the critical exponent  $\beta$  from the temperature dependence of the peak intensity,  $I_q(T)$ , at  $q = (\frac{1}{3}, \frac{1}{3}, 0)$ ,  $(\frac{1}{3}, \frac{1}{3}, 1)$  and  $(\frac{1}{3}, \frac{1}{3}, \frac{3}{2})$  using the relation,

$$M_q(T)^2 \propto I_q(T) - I_q^B = A(q) \left| 1 - \frac{T}{T_N} \right|^{2\beta}, \quad (3)$$

where  $M_q(T)$  denotes the magnetization with wave number  $q$ ,  $I_q^B$  represents the background intensity, and  $A(q)$  is the coefficient of the peak intensity at each  $q$ . We employed here the intensity at  $2\theta \approx 25^\circ$  (Fig. 5) as the background, since the intensity at this position does not depend on temperature.

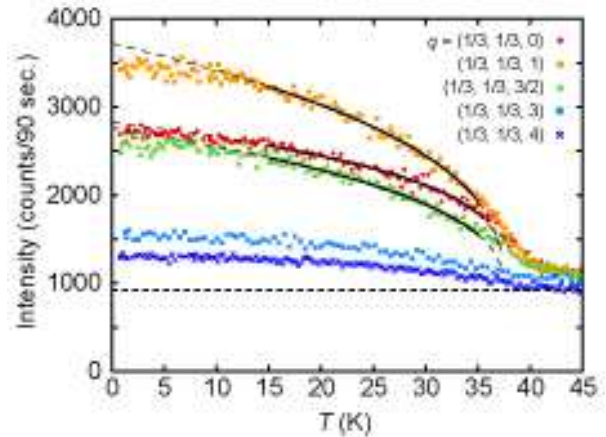


FIG. 6: (Color online) Temperature dependence of the peak intensity of the powder neutron diffraction at several  $q$  positions. The counting time is 90 sec. except for  $q = (\frac{1}{3}, \frac{1}{3}, 4)$ , for which it is 180 sec. The dotted line indicates the background,  $I_q^B = 920$  counts/90 sec. The curves represent the results of the fitting between 15 K and 35 K with Eq. (3) for the peaks at  $q = (\frac{1}{3}, \frac{1}{3}, 0)$ ,  $(\frac{1}{3}, \frac{1}{3}, 1)$ , and  $(\frac{1}{3}, \frac{1}{3}, \frac{3}{2})$ . The resulting critical exponent lies within the value  $\beta = 0.18 \pm 0.03$ .

To estimate  $I_q^B$  for the data in Fig. 6, we used the value multiplied by 1.5 to compensate for the different counting time between the  $2\theta$  scans (counts/60 sec.) and the temperature scans (counts/90 sec.). We used the fitting range from 15 K to 35 K in order to avoid the rounding region which is affected by the short-range spin fluctuation. The fitting yields  $0.18 \pm 0.03$ . This value is somewhat different from the previously reported value of  $\beta = 0.29$ ,<sup>23</sup> probably due to a different choice of  $T_N$ ; in the previous report, the authors used  $T_N = 40$  K, which was estimated from their neutron data itself, whereas we used  $T_N = 37.5$  K at which a clear anomaly is observed in other physical quantities. We believe that present choice of  $T_N$  is more appropriate.

## IV. DISCUSSION

In this section, we will first discuss the unusual critical behavior observed in the specific heat and neutron scattering measurements for  $\text{PdCrO}_2$ . Next we focus on the electrical resistivity exhibiting the characteristic sub-linear temperature dependence at temperatures above  $T_N$ .

### A. Critical behavior

Table I summarizes the obtained critical exponents for  $\text{PdCrO}_2$  and predicted values for various spin models. The exponent  $\alpha$  of  $\text{PdCrO}_2$  above  $T_N$  ( $t \leq 0.6$ ) is not consistent with the predicted value for the layered THAF,  $\text{SO}(3)$ .<sup>13</sup> Although the observed value is similar to that for the three-dimensional (3D) Ising-spin system, this model is not appropriate for  $\text{PdCrO}_2$  with Heisenberg spins in the quasi-2D crys-

TABLE I: Critical exponents  $\alpha$  and  $\beta$  of PdCrO<sub>2</sub> and the predicted values for various models.<sup>13,34,47</sup> The symbol SO(3) denotes the order-parameter space applicable to the case of the layered THAF. The exponents for VX<sub>2</sub> ( $X = \text{Cl, Br}$ ) are also presented. The symbol \* represents a cusp at  $T_N$ .

	$\alpha$	$\beta$
PdCrO <sub>2</sub> (above $T_N$ )	$0.13 \pm 0.02$	–
(below $T_N$ )	0*	$0.18 \pm 0.03$
Ising (2D, square lattice)	0 (log)	0.125
Ising (3D)	0.11	0.325
XY (3D)	–0.01	0.345
Heisenberg (3D)	–0.12	0.365
SO(3)	0.24	0.30
VCl <sub>2</sub> (Ref.16)	–	$0.20 \pm 0.02$
VBr <sub>2</sub> (Ref.17) (above $T_N$ )	0.59	–
(below $T_N$ )	0.28	$\sim 0.20$

tal structure. It should also be noted that the observed values of  $\alpha$  above and below  $T_N$  are clearly different. This is not consistent with the static scaling theories of the critical phenomena, which predict that both  $\alpha$  above and below the transition temperature should be identical.<sup>34,46</sup> This discrepancy is attributable to the extended critical region to temperatures above  $T_N$  due to spin frustration. The observed value of the exponent  $\beta$ , which is closely related to the staggered magnetization below  $T_N$ , agrees with those observed in VX<sub>2</sub> ( $X = \text{Cl, Br}$ ).<sup>16,17</sup> The main origin of the difference in  $\alpha$  between PdCrO<sub>2</sub> and VX<sub>2</sub> is probably due to the much narrower temperature range used for the fitting for VX<sub>2</sub>. In principle, one should distinguish the short range fluctuation observed in the wide temperature range above  $T_N$  from the critical fluctuation near  $T_N$ . However, our experimental results suggest that they are not separable in PdCrO<sub>2</sub>.

The critical behavior extending in wide temperature range above the magnetic transition temperature is observed not only in PdCrO<sub>2</sub> but also in other 2D-TL magnetic systems.<sup>42,48,49</sup> Interestingly, in such frustrated systems, diffuse neutron scattering is also visible in a similar temperature range.<sup>44,45</sup> This fact manifests that the critical state extending in a wide temperature range is one of the key features of the 2D-TL magnets.

### B. Metallic conductivity of PdCrO<sub>2</sub>

Here we discuss the temperature dependence of the electrical resistivity of PdCrO<sub>2</sub>, especially focusing on the  $T$ -sub-linear resistivity above  $T_N$ . For ordinary magnetic metals with non-frustrated localized spins, the contribution to the resistivity due to magnetic scattering between conduction electrons and the localized spins above their magnetic transition temperature is expected to be  $T$ -independent.<sup>38,39</sup> Therefore, the temperature dependence of the total resistivity above the mag-

netic transition temperature is  $T$ -linear mainly due to electron-phonon scattering.<sup>39</sup> Compared with such a case, the  $T$ -sub-linear resistivity observed in PdCrO<sub>2</sub> above  $T_N$  is unusual, and it indicates gradual reduction of the magnetic scattering from temperatures much above  $T_N$ . In the temperature range in which the  $T$ -sub-linear resistivity is found, the critical divergence is also observed in the magnetic specific heat and deviation from the Curie-Weiss behavior in the susceptibility. If one compares the insets of Fig. 2(b) and (c),  $d\rho/dT$  and  $d\chi/dT$  start to change at almost the same temperature. Moreover, the diffuse component in the neutron diffraction is observed above  $T_N$ , which suggests the development of short-range spin correlations. Thus, the unusual  $T$ -sub-linear resistivity of PdCrO<sub>2</sub> observed above  $T_N$  is attributable to the gradual development of short-range spin correlations, which may reduce the spin randomness and weaken the magnetic scattering of the conduction electrons.

The presence of conduction electrons may further lead to long-range interactions between spins, such as the Ruderman-Kittel-Kasuya-Yosida (RKKY) interaction. Such interactions may in turn compete with the short-range exchange interaction and affect the spin frustration. However, in PdCrO<sub>2</sub>, the conduction electrons do not seem to strongly affect the spin frustration, as evidenced by the 120° spin structure below  $T_N$  and the value of beta comparable to those of the corresponding insulators.

## V. CONCLUSION

In conclusion, we have investigated the 2D-HTAF compound PdCrO<sub>2</sub> by means of specific heat, electrical resistivity, magnetic susceptibility, and neutron scattering measurements. We found that PdCrO<sub>2</sub> exhibits metallic conductivity down to 0.35 K without chemical doping. We also confirmed the antiferromagnetic transition at  $T_N = 37.5$  K in the specific heat, which also affects the electrical resistivity. Powder neutron scattering measurements revealed that this compound forms a 120° spin structure with magnetic Bragg peaks of  $(\frac{1}{3}, \frac{1}{3}, l)$  and  $(\frac{2}{3}, \frac{2}{3}, l)$  with  $l = 0, \frac{1}{2}, 1, \frac{3}{2}, 2, \dots$  below  $T_N$ , similar to LiCrO<sub>2</sub>. Contributions due to diffuse scattering are strongly present even above  $T_N$ , which implies that the short-range spin correlations start to develop at temperatures much higher than  $T_N$ . Moreover, the magnetic Bragg peaks are broad even at temperatures much below  $T_N$ . This fact implies that coherence length of the ordered moments remain rather short.

In the magnetic specific heat we observed a critical behavior that extends in an unusually wide temperature range above  $T_N$ . Moreover, the critical exponents do not match with the exponents of standard models, and these are also strongly asymmetric above and below  $T_N$ . Such an extended and asymmetric critical region is attributed to the behavior characteristic of the frustrated Heisenberg spins on a triangular lattice.

In the electrical resistivity, we observed a sub-linear temperature dependence above  $T_N$ , which is quite different from the resistivity of ordinary magnetic metals with non-frustrated localized spins. This behavior is also characteristic of the conductive magnet with frustrated spins.

From the present study, it is still unclear whether or not the metallic conductivity affects the unusual critical phenomena. However, we found that the frustrated spins do affect the metallic conductivity of PdCrO<sub>2</sub>. Single crystal experiments in the future may allow us to extract the subtle effects of conduction on the geometrically frustrated spins.

### Acknowledgment

We would like to thank K. Ishida, M. Kriener, and S. Kitaka for useful discussions and for their assistance in measure-

ments. We also thank S. Maegawa, S. Fujimoto, S. Nakatsuji, and M. J. Lawler for fruitful discussions. This work was supported by the Grant-in-Aid for the Global COE Program “The Next Generation of Physics, Spun from Universality and Emergence” from the Ministry of Education, Culture, Sports, Science and Technology (MEXT) of Japan. It has also been supported by Grants-in-Aid for Scientific Research from MEXT and from the Japan Society for the Promotion of Science (JSPS).

- 
- \* Electronic address: takatsu@scphys.kyoto-u.ac.jp
- <sup>1</sup> G. H. Wannier, Phys. Rev. **79**, 357 (1950).
  - <sup>2</sup> N. D. Mermin and H. Wagner, Phys. Rev. Lett. **17**, 1133 (1966).
  - <sup>3</sup> P. W. Anderson, Mater. Res. Bull. **8**, 153 (1973).
  - <sup>4</sup> S. Teitel and C. Jayaprakash, Phys. Rev. B **27**, 598 (1983).
  - <sup>5</sup> S. Miyashita and H. Shiba, J. Phys. Soc. Jpn. **53**, 1145 (1984).
  - <sup>6</sup> H. Kawamura and S. Miyashita, J. Phys. Soc. Jpn. **53**, 4138 (1984).
  - <sup>7</sup> K. Kanoda, J. Phys. Soc. Jpn. **75**, 051007 (2006).
  - <sup>8</sup> D. H. Lee, J. D. Joannopoulos, J. W. Negele, and D. P. Landau, Phys. Rev. Lett. **52**, 433 (1984).
  - <sup>9</sup> H. Kawamura, J. Phys. Soc. Jpn. **53**, 2452 (1984).
  - <sup>10</sup> M. Yosefin and E. Domany, Phys. Rev. B **32**, 1778 (1985).
  - <sup>11</sup> D. H. Lee, J. D. Joannopoulos, J. W. Negele, and D. P. Landau, Phys. Rev. B **33**, 450 (1986).
  - <sup>12</sup> B. Berge, H. T. Diep, A. Ghazali, and P. Lallemand, Phys. Rev. B **34**, 3177 (1986).
  - <sup>13</sup> H. Kawamura, J. Phys. Condens. Matter **10**, 4707 (1998).
  - <sup>14</sup> H. Kawamura, J. Phys. Soc. Jpn. **56**, 474 (1987).
  - <sup>15</sup> H. Kawamura, J. Phys. Soc. Jpn. **61**, 1299 (1992).
  - <sup>16</sup> H. Kadowaki, K. Ubukoshi, K. Hirakawa, J. L. Martínez, and G. Shirane, J. Phys. Soc. Jpn. **56**, 4027 (1987).
  - <sup>17</sup> K. Takeda, N. Uryu, K. Ubukoshi, and K. Hirakawa, J. Phys. Soc. Jpn. **55**, 727 (1986).
  - <sup>18</sup> J. Wosnitza, R. Deutschmann, H. v Löhneysen, and R. K. Kremer, J. Phys. Condens. Matter. **6**, 8045 (1994).
  - <sup>19</sup> K. Momma and F. Izumi, J. Appl. Crystallogr. **41**, 653 (2008).
  - <sup>20</sup> M. Mekata, N. Yaguchi, T. Takagi, T. Sugino, S. Mituda, H. Yoshizawa, N. Hosoito, and T. Shinjo, J. Phys. Soc. Jpn. **62**, 4474 (1993).
  - <sup>21</sup> R. D. Shannon, D. B. Rogers, and C. T. Prewitt, Inorg. Chem. **10**, 713 (1971).
  - <sup>22</sup> J. P. Doumerc, A. Wichainchai, A. Ammar, M. Pouchard, and P. Hagenmuller, Mat. Res. Bull. **21**, 745 (1986).
  - <sup>23</sup> M. Mekata, T. Sugino, A. Oohara, Y. Oohara, and H. Yoshizawa, Physica B **213**, 221 (1995).
  - <sup>24</sup> H. Takatsu, H. Yoshizawa, and Y. Maeno, accepted in Journal of Physics: Conference Series (Proc. of Highly Frustrated Magnetism 2008).
  - <sup>25</sup> H. Takatsu, S. Yonezawa, S. Mouri, S. Nakatsuji, K. Tanaka, and Y. Maeno, J. Phys. Soc. Jpn. **76**, 104701 (2007).
  - <sup>26</sup> A. P. Ramirez, *Handbook of Magnetic Materials* (Elsevier Science, Amsterdam, 2001).
  - <sup>27</sup> A. P. Ramirez, G. P. Espinosa, and A. S. Cooper, Phys. Rev. B. **45**, 2505 (1992).
  - <sup>28</sup> S. Nakatsuji, Y. Nambu, H. Tonomura, O. Sakai, S. Honas, C. Broholm, H. Tsunetsugu, Y. Qiu, and Y. Maeno, Science **309**, 1697 (2007).
  - <sup>29</sup> T. Okuda, Y. Beppu, Y. Fujii, T. Onoe, N. Terada, and S. Miyasaka, Phys. Rev. B. **77**, 134423 (2008).
  - <sup>30</sup> N. Tristan, J. Hemberger, A. Krimmel, H. A. Krug vonNidda, V. Tsurkan, and A. Loidl, Phys. Rev. B **72**, 174404 (2005).
  - <sup>31</sup> J. S. Bernier, M. J. Lawler, and Y. B. Kim, arXiv:0801.0598v3.
  - <sup>32</sup> A. Kornblit, G. Ahlers, and E. Buehler, Phys. Lett. **43**, 531 (1973).
  - <sup>33</sup> B. J. C. van der Hoeven, D. T. Teaney, and V. L. Moruzzi, Phys. Rev. Lett. **20**, 719 (1968).
  - <sup>34</sup> H. E. Stanley, *Introduction to Phase Transitions and Critical Phenomena* (Oxford University press, New York, 1971).
  - <sup>35</sup> J. M. Ziman, *Electrons and Phonons* (Oxford University Press, New York, 1960).
  - <sup>36</sup> T. Moriya, *Spin Fluctuations in Itinerant Electron Magnetism* (Springer-Verlag, New York, 1985).
  - <sup>37</sup> T. Kasuya, Prog. Theor. Phys. **22**, 227 (1959).
  - <sup>38</sup> T. Kasuya, Prog. Theor. Phys. **16**, 58 (1956).
  - <sup>39</sup> K. Mori and K. Sato, J. Phys. Soc. Jpn. **49**, 246 (1980).
  - <sup>40</sup> K. Hirakawa, H. Ikeda, H. Kadowaki, and K. Ubukoshi, J. Phys. Soc. Jpn. **52**, 2882 (1983).
  - <sup>41</sup> A. Olariu, P. Mendels, F. Bert, B. G. Ueland, P. Schiffer, R. F. Berger, and R. J. Cava, Phys. Rev. Lett. **97**, 167203 (2006).
  - <sup>42</sup> L. K. Alexander, N. Buttgen, R. Nath, A. V. Mahajan, and A. Loidl, Phys. Rev. B **76**, 064429 (2007).
  - <sup>43</sup> H. Kadowaki, H. Takei, and K. Motoya, Phys. Cond. Matt. **7**, 6869 (1995).
  - <sup>44</sup> H. Kadowaki, H. Kikuchi, and Y. Ajiro, J. Phys. Cond. Matt. **2**, 4485 (1990).
  - <sup>45</sup> J. L. Soubeyroux, D. Fruchart, C. Dekmas, and G. L. Flem, J. Mag. Mag. Mater. **14**, 159 (1979).
  - <sup>46</sup> D. J. Amit, *Field Theory, the Renormalization Group, and Critical Phenomena* (World Scientific Publishing Co Pte Ltd, Singapore, 1978).
  - <sup>47</sup> J. C. LeGuillou and J. Zinn-Justin, Phys. Rev. Lett. **39**, 95 (1977).
  - <sup>48</sup> Y. Ajiro, H. Kikuchi, S. Sugiyama, T. Nakashima, S. Shamoto, N. Nakayama, M. Kiyama, N. Yamamoto, and Y. Oka, J. Phys. Soc. Jpn. **57**, 2268 (1988).
  - <sup>49</sup> H. Takeya, K. Ishida, K. Kitagawa, Y. Ihara, K. Onuma, Y. Maeno, Y. Nambu, S. Nakatsuji, D. E. MacLaughlin, A. Koda, and R. Kadono, Phys. Rev. B **77**, 054429 (2008).